Polymer Chemistry

PAPER

Check for updates

Redox-sensitive ferrocene functionalised double cross-linked supramolecular hydrogels†

Nikolai Liubimtsev, [a,b] Tom Kösterke,[a,b] Yunjiao Che,[a] Dietmar Appelhans, [a] Jens Gaitzsch *[a] and Brigitte Voit *[a,b]

Responsive double cross-linked hydrogels have proven to be a powerful approach to create smart polymer networks but unfold even greater potential if combined with supramolecular chemistry. A novel redox-sensitive ferrocene functionalised double cross-linked hydrogel is the core of this work. The explored network is based on poly(N-isopropylacrylamide) (PNiPAAm) and poly(2-methyl-2-oxazoline) (PMOXA) grafted chains with a β-cyclodextrin/ferrocene supramolecular host−guest system. A defined responsive behaviour was achieved using modified PMOXA macromonomers from a controlled synthesis, functionalised with β-cyclodextrin (CD-PMOXA) or with ferrocene (Fer-PMOXA), which were character-ised thoroughly by ^{1}H NMR, GPC, FTIR and Raman spectroscopy. The association affinity between host−guest macromonomers (CD-PMOXA and Fer-PMOXA) was investigated by DLS and 2D NOESY and ROESY NMR analysis. Additional redox responsive supramolecular host−guest complexes were included as bismacromonomers and acted as additional cross-linking points in the hydrogel. These reversible changes of the degree of cross-linking in the polymer network allowed for reversible swelling and shrink-age by dissociation and re-formation of the complex, which also influenced the rheology of the hydrogel. The reproducible swelling and rheological changes could be tailored by the number of supramolecular cross-linking points in the network as well as the chain length of PMOXA macromonomers. Connecting the changes in swelling behaviour with the mechanical characteristics allowed for deeper structural insights into the network. The adjustable supramolecular redox-sensitive double cross-linked hydrogel provides an opportunity for future applications, *e.g.* in microfluidics and diagnostics.

Introduction

One of the defining and key characteristic properties of cross-linked polymer networks is their ability to swell in a good solvent of network chains. A very prominent sub-type is hydro-gels that swell in an aqueous solution. When they are capable of distinctive changes of their properties upon an external stimulus provided in their environment, they are called respon-sive hydrogels. Responsive hydrogels are hence able to absorb and displace water in response to external stimuli (tempera-ture, solvent composition, pH, redox, light irradiation) that lead to a significant change in volume.[1–5] Despite the change in volume, these gels retain their original shape due to isotro-pic swelling. Based on the type of cross-linking, hydrogels can be divided into two categories: chemically cross-linked and physically cross-linked ones. Chemically cross-linked hydrogels possess covalent cross-linking points that allow varying of the mechanical properties of the polymer network by changing the density of the cross-linking points and they are commonly used when mechanically stable hydrogels are required.[6,7] At the same time, the permanent nature of this type of cross-linking point deprives it of possible reversible changes, where dynamic bonds would be required.[8] Physically cross-linked hydrogels possess non-covalent cross-linking points, which are based on physical interactions such as hydrogen bonds, van der Waals forces, and hydrophobic and coulombic inter-actions. Due to their non-covalent joints, physically cross-linked hydrogels show weak resistance to mechanical stimuli limiting the fields of their application. However, these types of networks can undergo reversible changes in network density based on the breakage and re-formation of physical bonds.[8]

Stronger non-covalent interactions can be achieved using dynamic supramolecular bonds, which can be broken and recovered by different chemical and physical stimuli. In recent years, the application of this type of bond as cross-linking points in hydrogels has drawn considerable and increasing attention.[9–11] Hydrogels based on such bonds have a stronger

[a]Leibniz-Institut für Polymerforschung Dresden e.V., Hohe Straße 6, 01069 Dresden, Germany. E-mail: gaitzsch@ipfdd.de, voit@ipfdd.de
[b]Technische Universität Dresden, Faculty of Chemistry and Food Chemistry, Organic Chemistry of Polymers, 01069 Dresden, Germany
†Electronic supplementary information (ESI) available. See DOI: 10.1039/d1py01211h

interaction than traditional physical bonds but are still not as strong as hydrogels with covalent cross-linking points.[12–14] Supramolecular chemistry exploiting reversible host–guest complexes is one of the most suitable methods to integrate dynamic bonds into hydrogels.[9,15] In this approach, dynamic host–guest complexes are widely applied as reversible cross-linking points to confer stimuli-responsive properties to the polymer materials.[10,16,17] Possible host–guest interactions include but are not limited to hydrogen bonding, hydrophobic forces, van der Waals forces, metal coordination, π–π interactions and electrostatic effects. Following this vast array of chemical interactions, host–guest complexes have become a popular tool in modern research on hydrogels and polymer science in general.[11,18,19]

Macrocyclic host–guest complexes with cyclodextrins (CDs), calix[n]arenes and cucurbit[n]urils are prominent examples for such non-covalent interactions.[20,21] These macrocyclic molecules have external hydrophilic groups and inner hydrophobic cavities which facilitate the interaction with different guest units such as adamantane, ferrocene, azobenzene, p-xylylene, and trimethylsilyl derivatives.[22–24] Among them, the β-cyclodextrin (β-CD)/ferrocene host–guest complex is commonly used to confer redox sensitivity to the system.[25] It is known that ferrocene and β-CD can form a 1:1 complex in aqueous solution (association constant 17×10^3 M),[1,26–28] which can be reversibly destroyed and re-formed over various cycles by oxidation and reduction of ferrocene to the ferrocenium ion and *vice versa*.[29] The high degree of reversibility allowed for an application in self-healing hydrogels by Peng *et al.*[30] and the good biocompatibility of the system allowed for application in tissue engineering and use as a carrier for drug delivery by Zhang *et al.*[31] Since breaking and re-forming the complex can lead to significant changes in volume, Nakahata *et al.* were able to create a supramolecular hydrogel actuator based on the complex between β-CD and ferrocene.[14]

However, the drawback of the weak control of swelling/mechanical behaviour at the swollen state restricts the development of hydrogels based on supramolecular chemistry. Double cross-linked hydrogels, bearing both covalent and dynamic cross-linking points, are promising candidates to overcome the drawback just mentioned. The covalent cross-linking points permanently maintain the network, whereas the dynamic cross-linking points are able to realise the responsive and reversible swelling behaviour of a hydrogel through cleavage and re-formation. From our previous study of double cross-linked grafted hydrogels based on a β-CD/adamantane host–guest complex,[32] we now transferred our knowledge to the β-CD/ferrocene supramolecular complex (Fig. 1). Due to redox sensitivity and controlled mechanical behaviour secured by the presence of covalent cross-linking points, hydrogels with the β-CD/ferrocene complex are a promising system for various applications like the capture and release of molecules in microfluidics. The chosen host–guest complex is redox responsive and in that respect similar to the equally responsive disulphide bonds used in double cross-linked hydrogels in an earlier study.[33] Exploiting the host–guest system enables the use of different redox chemicals and most importantly allows the fine-tuning of the viscoelastic response of the hydrogel by tuning the length of the PMOXA in the bismacromonomers integrated into the hydrogel.

Here, we report on a novel double cross-linked hydrogel with a poly(N-isopropylacrylamide) (PNiPAAm) backbone cross-linked with N,N'-methylenebis(acrylamide) (BIS) as a permanent cross-linker and β-CD/ferrocene host–guest complexes as reversible cross-linking points. It should be noted that initial experiments with acrylamide did not form stable hydrogels. Poly(2-methyl-2-oxazoline) (PMOXA) bismacromonomers were used to introduce the host and guest molecules as part of additional cross-linking chains when the complex is present. Upon breaking the complex, the material is transformed into a hydrogel with grafted side chains (Fig. 1). In recent years, the number of publications that used PMOXA has increased dramatically due to its biocompatibility as well as the facility of the development of a clearly defined polymer structure by controlled polymerisation.[34,35] PMOXA macromonomers with different chain lengths (n = 30, 37) and varying functionalities (alkyne (Alk-n), ferrocene (Fer-n), and β-CD (CD-n)) were synthesised *via* living cationic ring-opening polymerisation. The
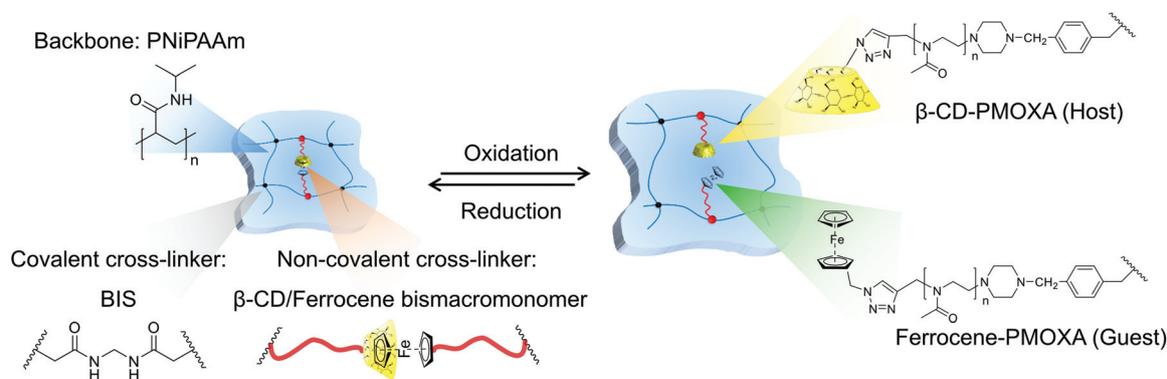
Fig. 1 Redox-sensitive ferrocene functionalised double cross-linked supramolecular hydrogel and chemical structure of PMOXA macromonomers, which were used for the hydrogel synthesis.

well-defined PMOXA macromonomer structures were investigated by ^{1}H NMR and GPC, and the successful coupling of host and guest moieties with PMOXA was evaluated by ^{1}H NMR, FTIR and Raman spectroscopy. The β-CD/ferrocene complex was studied by DLS and 2D NOESY and ROESY NMR. Following the synthesis of various hydrogels *via* free radical polymerisation in methanol, the viscoelastic properties of the gels were probed using the degree of swelling and rheology. The presence of additional functional host–guest cross-linking points allows the repeated swelling and shrinking of the gel by dissociating and re-forming of host–guest complex using the redox stimulus. Variation of the number of supramolecular bismacromonomers in the network as well as the chain length of PMOXA macromonomers with Fer and β-CD end groups allows the tailoring of the mechanical properties of the hydrogels.

Experimental section

Materials

Propargyl *p*-toluenesulfonate (p-OTs, Sigma-Aldrich, 97%) and methyl trifluoromethanesulfonate (MeOTf, Sigma-Aldrich, 98%) were purified by distillation and stored under an argon atmosphere prior to use. 2-Methyl-2-oxazoline (MOXA, Sigma-Aldrich, 98%) was distilled under argon before use. *N*-Isopropylacrylamide (TCI, stabilised with MEHQ) was recrystallised in *n*-hexane, and *N,N*-diisopropylethylamine (DIPEA, Sigma-Aldrich, 98%) was distilled and stored under argon. Methanol (Sigma-Aldrich, 99.8%), chloroform (Fisher Scientific, 99.8%), acetonitrile (MeCN, Sigma-Aldrich, 99.8%), piperazine (Sigma-Aldrich), 4-vinylbenzyl chloride (Sigma-Aldrich, 90%), 2,6-di-*tert*-butyl-4-methylphenol (Sigma-Aldrich), 6-monoazido-6-monodeoxy-*b*-cyclodextrin (Cyclodextrin-Shop), ferrocenemethanol (Sigma-Aldrich, 97%), sodium azide (Sigma-Aldrich), *N,N'*-methylenebis(acrylamide) (BIS, Sigma-Aldrich, 99%), azobisisobutyronitrile (AIBN, Sigma-Aldrich, 98%), and copper(ı) iodide (Sigma-Aldrich, 98%) were used as received.

Synthesis

Vinylating agent *N*-(4-vinylbenzyl)piperazine (VBP). VBP was synthesised according to the literature[36] with minor changes. Briefly, the synthesis of the vinylating agent proceeded as follows. Piperazine (7.80 g, 90.70 mmol, 6.00 eq.) and 4-vinylbenzyl chloride (2.13 mL, 15.1 mmol, 1.00 eq.) were dissolved in anhydrous chloroform (120 mL) at 0 °C. Next, a trace amount of a stabilizer 2,6-di-*tert*-butyl-4-methylphenol (33.40 mg, 0.15 mmol, 0.01 eq.) was added to the solution. The solution was stirred at room temperature (RT) overnight. Then, the precipitated white solid was removed by filtration and the organic phase was concentrated to 100 mL. The organic solution was extracted with 250 mL of water 7 times and dried over Na$_2$SO$_4$. Chloroform was removed under vacuum. Thus, VBP in the form of a yellow oil was obtained (yield 2.01 g, 66%).

^{1}H NMR (500 MHz, CDCl$_3$): δ = 2.39 ppm (br. s., 4 H), 2.86 ppm (t, *J* = 4.9 Hz, 4 H), 3.46 ppm (s, 2 H), 5.20 ppm (d, *J* = 11.0 Hz, 1 H), 5.71 ppm (d, *J* = 17.7 Hz, 1 H), 6.69 ppm (dd, *J* = 17.5, 10.9 Hz, 1 H), 7.22–7.29 ppm (m, 2 H), 7.30–7.37 ppm (m, 2 H).

Alkynyl-PMOXA$_{37}$-VBP (Alk-37). PMOXA was synthesised *via* living cationic ring-opening polymerisation (CROP) of 2-methyl-2-oxazoline. The synthesis conditions were similar to those described earlier.[32] Briefly, under an argon atmosphere, p-OTs (165 μL, 0.95 mmol, 0.025 eq.) was dissolved in dry acetonitrile (9 mL), followed by adding distilled MOXA (3.00 mL, 38.10 mmol, 1.00 eq.). Then the solution was heated at 70 °C and stirred for 3.5 h. After the cooling to RT, terminating agent VBP (578 mg, 2.86 mmol, 0.075 eq.) was added, and the solution was stirred for 24 h at RT. Then anhydrous K$_2$CO$_3$ (460 mg, 3.33 mmol, 0.087 eq.) was added, and the solution was stirred for 24 h. The purification steps proceeded as follows. First, the suspension was centrifuged twice, the organic phase was filtered using a 0.2 μm PTFE syringe filter and removed under vacuum. Then the product was precipitated twice in diethyl ether (250 mL) at 0 °C. The final product was obtained after dialysis (3 days) against methanol with regenerated cellulose membrane of MWCO = 1000 (Carl Roth GmbH, Germany) to remove the excess VBP followed by high-vacuum freeze drying (Alpha 1–2 LDplus, Martin Christ, Germany) as a white powder with 43% yield (1.50 g).

^{1}H NMR (500 MHz, CDCl$_3$): δ = 2.02–2.20 ppm (m, 111 H), 2.39–2.56 ppm (m, 8 H), 2.75–2.92 ppm (m, 1 H), 3.47 ppm (d, *J* = 17.3 Hz, 147 H), 4.02–4.36 ppm (m, 2 H), 5.22 ppm (d, *J* = 10.7 Hz, 1 H), 5.73 ppm (d, *J* = 17.7 Hz, 1 H), 6.70 ppm (dd, *J* = 17.7, 11.0 Hz, 1 H), 7.26 ppm (d, *J* = 7.8 Hz, 2 H), 7.36 ppm (d, *J* = 7.9 Hz, 2 H).

GPC: M_n = 3400 g mol^{-1}, Đ = 1.15.

Alkynyl-PMOXA$_{30}$-VBP (Alk-30). Macromonomers with shorter chain length (30 repeating units) were synthesised with 30 eq. of MOXA. Reaction time was adjusted to 3 h. The purification process was the same as for Alk-37. Alk-30 was further used for CD-30 and Fer-30 synthesis (yield 1.22 g, 35%).

^{1}H NMR (500 MHz, CDCl$_3$): δ = 2.01–2.27 ppm (m, 90 H), 2.37–2.60 ppm (m, 8 H), 2.75–2.91 ppm (m, 1 H), 3.48 ppm (d, *J* = 11.0 Hz, 120 H), 4.03–4.36 ppm (m, 2 H), 5.22 ppm (d, *J* = 10.4 Hz, 1 H), 5.73 ppm (d, *J* = 17.7 Hz, 1 H), 6.70 ppm (dd, *J* = 17.5, 10.9 Hz, 1 H), 7.26 ppm (d, *J* = 7.3 Hz, 2 H), 7.35 ppm (d, *J* = 7.3 Hz, 2 H).

GPC: M_n = 2800 g mol^{-1}, Đ = 1.14.

Methyl-PMOXA$_{35}$-VBP (Me-35). The methyl-PMOXA macromonomer was synthesised similar to the alkynyl-PMOXA macromonomer using methyl trifluoromethanesulfonate (34 μL, 0.30 mmol, 0.025 eq.) as the initiator and 2-methyl-2-oxazoline (1.00 mL, 12.00 mmol, 1.00 eq.) in MeCN (3 mL). The reaction conditions were defined as 1 h 20 min at 85 °C. The purification process was the same as for Alk-37. The resulting macromonomer was obtained as a white powder (yield 281 mg, 26%).

^{1}H NMR (500 MHz, CDCl$_3$): δ = 2.01–2.16 ppm (m, 105 H), 2.37–2.57 ppm (m, 8 H), 2.70–3.05 ppm (m, 3 H), 3.30–3.55 ppm (m, 142 H), 5.19 ppm (d, *J* = 10.0 Hz, 1 H), 5.70 ppm (d, *J* = 15.0 Hz, 1 H), 6.67 ppm (dd, *J* = 20.0, 10.0 Hz,

1 H), 7.23 ppm (d, J = 5.0 Hz, 2 H), 7.32 ppm (d, J = 5.0 Hz, 2 H).

GPC: M_n = 2900 g mol^{-1}, $Đ$ = 1.11.

β-Cyclodextrin-PMOXA$_{37}$-VBP (CD-37). Under an argon atmosphere, mono-6-azido-6-deoxy-beta-cyclodextrin (138 mg, 119 µmol, 1.00 eq.) was dissolved in a mixture of water (1 mL) and acetonitrile (1 mL), followed by adding diisopropylethylamine (2.00 µm, 12.30 µmol, 0.11 eq.) and copper(I) iodide (2.39 mg, 12.50 µmol, 0.11 eq.) and Alk-37 (401 mg, 118 µmol, 1.00 eq.). Then the solution was stirred for 3 days at RT. The solvent was removed under vacuum and the crude product was purified by dialysis against distilled water with regenerated cellulose membrane of MWCO = 1000 (Carl Roth GmbH, Germany) for three days. The pure product CD-37 was obtained after high-vacuum freeze drying (Alpha 1–2 LDplus, Martin Christ, Germany) as a slightly bluish powder with 61% yield (328 mg).

^{1}H NMR (500 MHz, DMSO-d$_6$): δ = 1.92–2.05 ppm (m, 111 H), 2.31–2.45 (m, 8 H), 3.32–3.51 ppm (m, 148 H), 3.54–3.71 ppm (m, 21 H), 4.39–4.51 ppm (m, 6 H), 4.55 ppm (br. s., 2 H), 4.74–4.90 ppm (m, 7 H), 5.22 ppm (d, J = 10.7 Hz, 1 H), 5.61–5.75 ppm (m, 14 H), 5.79 ppm (d, J = 17.7 Hz, 1 H), 6.71 ppm (dd, J = 17.5, 10.9 Hz, 1 H), 7.25 ppm (d, J = 7.6 Hz, 2 H), 7.41 ppm (d, J = 7.6 Hz, 2 H), 7.86 ppm (s, 1 H).

GPC: M_n = 4600 g mol^{-1}, $Đ$ = 1.14.

CD-30: Alk-37 was replaced by Alk-30 but keeping the equivalents (yield 336 mg, 84%).

Azidomethylferrocene. Azidomethylferrocene was synthesised from ferrocenemethanol according to the literature.[37] Briefly, the solution of ferrocenemethanol (1.00 g, 4.63 mmol, 1.00 eq.) and sodium azide (1.81 g, 27.80 mmol, 6.00 eq.) in glacial acetic acid (60 mL) was heated at 50 °C and stirred for 3 h. Then the solution was diluted in CH$_2$Cl$_2$ (200 mL) and the organic phase was washed with a saturated solution of NaHCO$_3$ (3 × 250 mL) and dried over Na$_2$SO$_4$. CH$_2$Cl$_2$ was removed under vacuum. The product was purified by column chromatography (EtOAc–n-hexane 1 : 25). The product was obtained as a brown-red crystalline solid with 97% yield (1.08 g).

^{1}H NMR (500 MHz, CDCl$_3$): δ = 4.13 ppm (s, 2 H), 4.18 ppm (s, 5 H), 4.21 ppm (s, 2 H), 4.25 ppm (s, 2 H).

Ferrocene-PMOXA$_{37}$-VBP (Fer-37). Under an argon atmosphere, azidomethylferrocene (30.00 mg, 124 µmol, 1.00 eq.) was dissolved in dry acetonitrile (1.3 mL), followed by adding diisopropylethylamine (2.20 µm, 12.40 µmol, 0.10 eq.) and copper(I) iodide (2.41 mg, 12.60 µmol, 0.10 eq.) and Alk-37 (422 mg, 124 µmol, 1.00 eq.). Then the solution was stirred for 3 days at RT. The solvent was removed under vacuum and the crude product was purified by dialysis against methanol with regenerated cellulose membrane of MWCO = 1000 (Carl Roth GmbH, Germany) for three days. The pure product CD-37 was obtained after high-vacuum freeze drying (Alpha 1–2 LDplus, Martin Christ, Germany) as a yellow powder with the 56% yield (251 mg).

^{1}H NMR (500 MHz, DMSO-d$_6$): δ = 1.89–2.07 ppm (m, 111 H), 2.27–2.46 ppm (m, 8 H), 3.33–3.60 ppm (m, 148 H),

4.17 ppm (d, J = 3.8 Hz, 7 H), 4.33 ppm (br. s., 2 H), 4.43–4.62 ppm (m, 2 H), 5.18–5.36 ppm (m, 3 H), 5.79 ppm (d, J = 17.7 Hz, 1 H), 6.71 ppm (dd, J = 17.5, 10.9 Hz, 1 H), 7.25 ppm (d, J = 7.3 Hz, 2 H), 7.41 ppm (d, J = 7.9 Hz, 2 H), 7.94–7.85 ppm (m, 1 H).

GPC: M_n = 3600 g mol^{-1}, $Đ$ = 1.09.

Fer-30: Alk-37 was replaced by Alk-30 but keeping the equivalents (yield 144 mg, 42%).

Ada-40: (Adamantane-PMOXA$_{40}$-VBP) was synthesised as described previously.[30]

Hydrogel synthesis. The hydrogels were synthesised *via* free radical polymerisation in methanol (0.93 mL). For the synthesis of GH-37a, NiPPAm (150 mg, 1.33 mmol, 16 wt%) as monomer, BIS (1.02 mg, 6.63 µmol, 0.5 mol%) as the covalent cross-linker, the host and guest bismacromonomers (30.60 mg, 6.73 µmol, 0.5 mol% (CD-37) and 24.30 mg, 6.72 µmol, 0.5 mol% (Fer-37)) as a reversible redox-sensitive non-covalent cross-linker and AIBN (2.18 mg, 13.27 µmol, 1 mol%) as an initiator were used. Prior to the hydrogel formation, the ferrocene and β-CD macromonomers were dissolved in methanol, heated at 40 °C and stirred for 24 h for complete complex formation. Afterward NiPAAm, BIS and AIBN were added to the solution with bismacromonomers and the solution was transferred to a glass vessel with an internal diameter of 6.5 mm. The polymerisation of the hydrogel was carried out in the oven at 50 °C for 24 h. After 3 days of washing in deionised water (steadily exchanging deionised water to remove all MeOH), the homogeneous and yellow ferrocene-containing hydrogels and colourless control hydrogels were obtained.

This procedure was altered as follows for the other hydrogels:

GH-37b: BIS was altered (2.04 mg, 13.25 µmol, 1 mol%)

GH-37c: CD-37 was altered (61.1 mg, 13.4 µmol, 1 mol%) and Fer-37 was altered (48.5 mg, 13.4 µmol, 1 mol%)

GH-30: CD-37 was replaced by CD-30 (26.30 mg, 6.65 µmol, 0.5 mol%) and Fer-37 was replaced by Fer-30 (20.20 mg, 6.65 µmol, 0.5 mol%)

GH-35Me: CD-37 and Fer-37 were left out, but Me-35 (48.03 mg, 13.25 µmol, 1 mol%) was added. The synthesis was carried out in 0.74 mL of distilled water using sodium persulfate (8 µL, 13.25 µmol, 1 mol%) and tetramethylethylenediamine (1 µL, 13.25 µmol 1 mol%) at RT.

Pure PNiPAAm network: CD-37 and Fer-37 were left out.

Characterisation

NMR and 2D NOESY and ROESY NMR spectroscopy. [1]H spectra were recorded on a Bruker Avance III 500 spectrometer (500.13 MHz) using chloroform-d or DMSO-d$_6$ as the solvent at RT. 2D NOESY and ROESY NMR spectra were obtained using D$_2$O or methanol-d$_4$ as a solvent at 30 °C (NOESY 1.00 s, ROESY 0.99 s). All the spectra were calibrated to the residual signal of the deuterated solvent. Before measurement, the host–guest complex was prepared as follows: an aqueous solution of macromonomers was stirred for 24 h at 70 °C for D$_2$O and at 40 °C for methanol-d$_4$. In the evaluation, the ppm

values for the chemical shift δ were rounded to two decimal places and the values of the coupling constant J (in Hz) to one decimal place. The number of hydrogen atoms determined by integration is also given. The signal of the solvent served as the internal standard. The abbreviations s = singlet, d = doublet, t = triplet, m = multiplet and br. = broad are used throughout.

Gel permeation chromatography (GPC). GPC measurements were performed on SECcurity[2] (PSS), equipped with GRAM Precolumn, Gram 30 Å, Gram 3000 Å columns under the following conditions: eluent – DMAc (5 g l^{-1} LiBr and 1% H$_2$O) at 50 °C, the injection volume was adjusted to 100 µL and the selected flow rate to 1 mL min^{-1}. Before the measurement, the system was calibrated against PMOXA initiated with methyltriflate and terminated with piperidine.

Fourier transform infrared spectroscopy (FTIR). The FTIR spectra of the macromonomers were recorded on a Vertex 80v instrument (Bruker) in the range of 4000–600 cm^{-1} with 100 scans at a resolution of 4 cm^{-1}. Analysis of the results was performed under baseline normalisation and correction using the OPUS 7 software (Bruker).

RAMAN spectroscopy. Raman spectra of macromonomers were acquired using Raman imaging system WITEC alpha300R (WITec GmbH, Germany), which was generated by a pulsed 532 nm laser (laser power: 3–10 mW, integration time: 0.5 s, zoom: 20×).

Dynamic light scattering (DLS). The hydrodynamic diameter of the macromonomers was recorded on a Zetasizer Nano ZS instrument (Malvern Instruments, UK), equipped with a He–Ne laser (4 mW, l = 633 nm) at a fixed angle of 1731 (noninvasive backscatter (NIBS) mode). The results were analysed using the Zetasizer software. Before measurement, the host–guest complex was prepared as follows: an aqueous solution of macromonomers was stirred 24 h at 70 °C.

Scanning electron microscopy (SEM). The hydrogels were analysed using an Ultra 55 PLUS field emission scanning electron microscope (Carl Zeiss AG, Germany) at 3 kV (magnification: 1000×). The SEM samples were freeze-dried, cut into suitable dimensions and sputter-coated with platinum before the measurement.

Swelling characteristics of hydrogels

For the swelling measurement, the respective hydrogel was prepared as an approximate 5 mm thick slice from the cylindrical hydrogel obtained after synthesis. In the first step, the initial mass value was always recorded. For this purpose, the hydrogel was taken out of the aqueous medium and carefully dried with a lint-free cloth. A glass plate was used as a wafer for hydrogels when measuring the mass on the balance. The redox cycles were then carried out in a flask with a volume of 25 mL. The hydrogel was treated with about 25 mL of the 0.1 mM hydrogen peroxide solution in a vessel. Then, the hydrogel was taken out, washed with water, and placed in the vessel with water (25 mL) for further swelling duration. Afterwards, the measurement of the mass took place as described before. In addition, the diameter and height of the

hydrogel slice were recorded for each measuring point. The same procedure was followed for the reductive step, except that a 10 mM sodium thiosulfate solution was used. This procedure was used to investigate the swelling properties of the different hydrogels.

Rheology

For the rheological measurement of the hydrogels, the Advanced Rheometric Expansion System (ARES) (TA-Instrument) was used. The stainless steel plates with a diameter of 25 mm were calibrated in advance and the axial force was zeroed. Then the hydrogel was fixed between two parallel aligned stainless steel plates at RT. The previously measured hydrogel data such as the diameter and height were entered into the device for the calculations of the storage module G'. The exact determination of the diameter is crucial here. Therefore, this is measured at different points on the hydrogel slice. After the hydrogel was fixed into the rheometer at a force of 5 g, the measurement started. The storage modulus G' was examined at an oscillating frequency of 1.0 to 100 rad s^{-1} and a strain range of 2%. This strain was in the range of linear viscoelasticity as indicated by the flat G' and G'' over the entire frequency range (Fig. S15†).

Results and discussion

Polymer synthesis

The initial step of this work was the synthesis of bisfunctional PMOXA macromonomers (Fig. 2 and Fig. S1†). Using a propargyl tosylate initiator, an alkyne group was included into the PMOXA chains (Alk-n) and the CROP reactions were terminated with the vinylating agent N-(4 vinylbenzyl)piperazine (VBP) (Fig. 2a). VBP was essential to introduce a polymerising group and thus to be able to use the PMOXA chains as macromonomers during the hydrogel formation later on. The alkyne group was the basis for future modifications using the azide–alkyne click reaction. In order to study the influence of the chain length, a longer alkyne-PMOXA of around 40 repeating units and a shorter alkyne-PMOXA of around 30 repeating units (Alk-30) were targeted. Similar steps in polymer synthesis have been described in detail in our previous study.[32]

The vinylating agent VBP which was used as the terminating agent in all PMOXA syntheses, was successfully derived from piperazine and 4-vinylbenzyl chloride according to the literature (confirmed by ^{1}H NMR, Fig. S2†).[36] PMOXA was synthesised via living CROP of 2-methyl-2-oxazoline with a ratio of [monomer] : [initiator] = 40 : 1 in acetonitrile at 70 °C for 3.5 h. After their synthesis, the macromonomers were purified by dialysis against MeOH. The chemical structure of the final polymer was investigated by ^{1}H NMR, which was also used to determine the degree of polymerisation (Fig. 2a). The signals δ = 2.81 ppm (integral = 1.00) and δ = 4.01–4.20 ppm (integral = 2.00, Fig. 2a, blue) of the ^{1}H NMR spectra of the polymer refer to the alkynyl protons and methylene protons in the initiator respectively. Their presence in the polymer con-
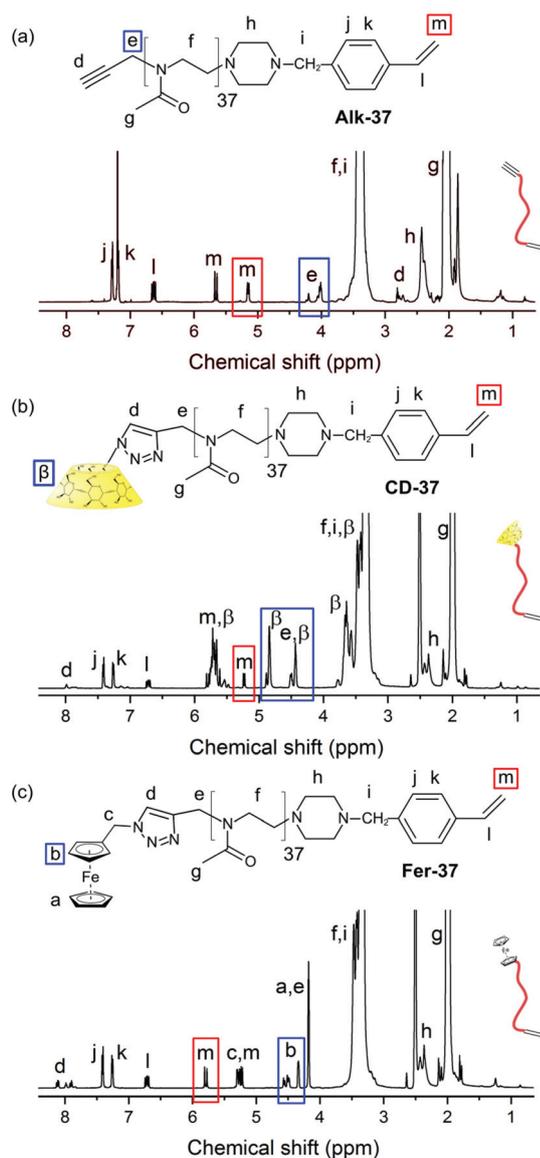
Fig. 2 ^{1}H NMR spectra of PMOXA macromonomers. (a) ^{1}H NMR spectrum of alkyne PMOXA (Alk-37) recorded in CDCl₃, (b) ^{1}H NMR spectrum of CD-PMOXA (CD-37) recorded in DMSO-d₆, (c) ^{1}H NMR spectrum of Fer-PMOXA (Fer-37) recorded in DMSO-d₆.

firmed the successful connection of the initiator to the macromonomers. From the integrating ratio of the signals corresponding to methylene protons and terminal ethylene proton (δ = 4.01–4.20 ppm, integral = 2.00, Fig. 2a, blue; δ = 5.14 ppm, integral = 1.00, Fig. 2a, red), the end-group functionality (EGF) of PMOXA with VBP was 99%. The high functionality with VBP allowed achieving a high degree of integration of macromonomers in the process of hydrogel synthesis. Analysing the integral ratio to the one of the PMOXA backbone peaks (δ = 3.04–3.66 ppm, "f" in Fig. 2a–c and Fig. S3†) gave the degree of polymerisation (DP) of 37, confirming the presence of Alk-37 (M = 3400 g mol⁻¹, Table 1) (for Alk-37: integral ratio of methylene protons δ = 4.01–4.20 ppm, integral = 2.00 and PMOXA backbone δ = 3.04–3.66 ppm, integral = 147.00). A DP of Alk-37 is close to the theoretical value confirming good adjustment of molar weight during the synthesis. The shorter PMOXA chains were synthesised using a 30 : 1 monomer : initiator ratio, yielding a DP of 30 (Alk-30; integral ratio δ = 4.01–4.20 ppm, integral = 2.00 and PMOXA backbone δ = 3.04–3.66 ppm, integral = 120.00) and had an equal EGF with VBP. GPC analysis revealed the expected monomodal distribution and low dispersities of 1.15 and 1.14 for Alk-37 and Alk-30, respectively (Table 1). Polymers for control experiments were synthesised as well. In order to test hydrogels with no host–guest complex, a methyl-terminated version with a DP of 35 was synthesised (Me-35). Since the β-cyclodextrin/adamantane host–guest complex is stronger than the one with ferrocene,[38] an adamantane-functionalised PMOXA with a DP of 40 (Ada-40) was synthesised following a previously published protocol.[32] This polymer was intended to displace ferrocene in all host–guest complexes to gain a reference material in characterisation experiments.

CD-PMOXA and Fer-PMOXA macromonomers were obtained from Alk-PMOXA with a following copper catalysed azide–alkyne click reaction (CuAAC) with β-CD-N₃ and Fer-N₃, respectively. Generally, the azide derivatives (1 eq.) and Alk-PMOXA (1 eq.) were used in the presence of DIPEA and CuI under argon in acetonitrile (for Fer-N₃) in acetonitrile/water (for β-CD-N₃) to implement the transition from alkynyl group to the triazole ring. In case of the CD derivatives, for the separation of the CD-PMOXA macromonomer from the free β-CD-N₃ molecules and copper catalysts, dialysis against water was performed. The obtained CD-37 and CD-30 were analysed by

Table 1 Synthesis data and characteristics of poly(2-methyl-2-oxazoline) macromonomers

Polymer	[Monomer]/[initiator]	$M_{n,th}$[a] [g mol⁻¹]	$M_{n,NMR}$[b] [g mol⁻¹]	$M_{n,GPC}$[c] [g mol⁻¹]	$Đ$[c]	EGF[b] (%)
Alk-37	40 : 1	3600	3400	2400	1.15	99
Fer-37		3800	3600	2600	1.09	98
CD-37		4800	4600	2800	1.14	94
Alk-30	25 : 1	2400	2800	2200	1.14	99
Fer-30		2600	2900	2200	1.19	99
CD-30		3500	3800	2800	1.23	97
Me-35	40 : 1	3600	3200	2900	1.11	98
Ada-40	40 : 1	3900	4100	3600	1.18	98

[a] Calculated from [monomer] : [initiator]. [b] End-group functionality determined by ^{1}H NMR spectroscopy. [c] Determined by GPC in DMAc.

^{1}H NMR and GPC (Fig. 2b, Table 1 and Fig. S4, S10†). The EGF after CuAAC was calculated ($EGF_{CD-37} = 94\%$ and $EGF_{CD-30} = 97\%$) from the signals corresponding to the terminal ethylene proton and signals from β-CD ($\delta = 5.14$ ppm, integral = 1.00, Fig. 2b, red; $\delta = 4.50$–4.75 ppm, integral = 16.00, Fig. 2b, blue; Fig. S4†). Further confirmation of the successfully conducted CuAAC was provided from FTIR analysis of β-CD-N$_3$ and CD-PMOXA macromonomer (Fig. S8†). After CuAAC, the IR peak attributed to the azido group at 2068 cm^{-1} disappeared and new signals corresponding to the carbonyl stretching vibration and carbon–nitrogen bond appeared at 1615 cm^{-1} and 1030 cm^{-1}, respectively. Raman spectroscopy indicated the peak at 2117 cm^{-1} corresponding to the alkyne group and its disappearance after the reaction. GPC data showed increased molecular weight and slightly increased dispersity of CD-30 compared with Alk-30 (Table 1 and Fig. S10†). Summarising the results from NMR, GPC, FTIR and Raman spectroscopy it can be stated that the coupling of Alk-PMOXA with β-CD was effectively carried out. The synthesis of ferrocene macromonomers was implemented by two steps. First, ferrocenemethanol (Fer-OH) was converted into azidomethylferrocene (Fer-N$_3$) according to the literature and proven by FTIR and ^{1}H NMR (Fig. S7 and S8†).[37] Similar to CD-PMOXA, the ferrocene macromonomers (Fer-37 and Fer-30) were obtained via CuAAC and analysed by ^{1}H NMR and (Fig. 2c, Table 1 and Fig. S5, S10†). The EGF after CuAAC was calculated ($EGF_{Fer-37} = 98\%$ and $EGF_{Fer-30} = 99\%$) from the signals corresponding to the terminal ethylene proton and signals from ferrocene ($\delta = 5.67$ ppm, integral = 1.00, Fig. 2c, red; $\delta = 4.55$–4.23 ppm, integral = 3.90, Fig. 2c, blue, Fig. S5†). FTIR and Raman spectroscopy confirmed the successful connection of azidomethylferrocene to Alk-PMOXA (Fig. S8 and S9†). GPC showed a slightly altered dispersity within the macromonomer series (Table 1 and Fig. S10†), but still monomodal distribution of each macromonomer. The high functionality with host and guest agents potentially allowed for a high degree of supramolecular cross-linking density of the intended hydrogels. This would also mean a notable response to redox stimuli of the hydrogels following the introduction of non-permanent cross-linking points.

Host–guest complex study

With the macromonomers in-hand, the next step was to study the β-CD/ferrocene host–guest complex forming the bismacromonomer, i.e. the reversible cross-linker. Knowing the association affinity of the synthesised macromonomers (CD-PMOXA and Fer-PMOXA) was the key characteristic before the hydrogel formation could be started. To investigate the coupling of ferrocene and β-CD macromonomers, DLS and 2D NOESY and ROESY NMR were conducted. DLS gave the hydrodynamic radius including the distribution of the macromonomers CD-PMOXA and Fer-PMOXA and their mixture (1 : 1 eq.) in water at 25 °C. The hydrodynamic diameter increased from 5.2 nm (CD-PMOXA) and 5.4 nm (Fer-PMOXA) to 8.1 nm for their mixture due to the formation of the host–guest complex (Fig. 3a). In addition to DLS measurement, 2D NOESY and
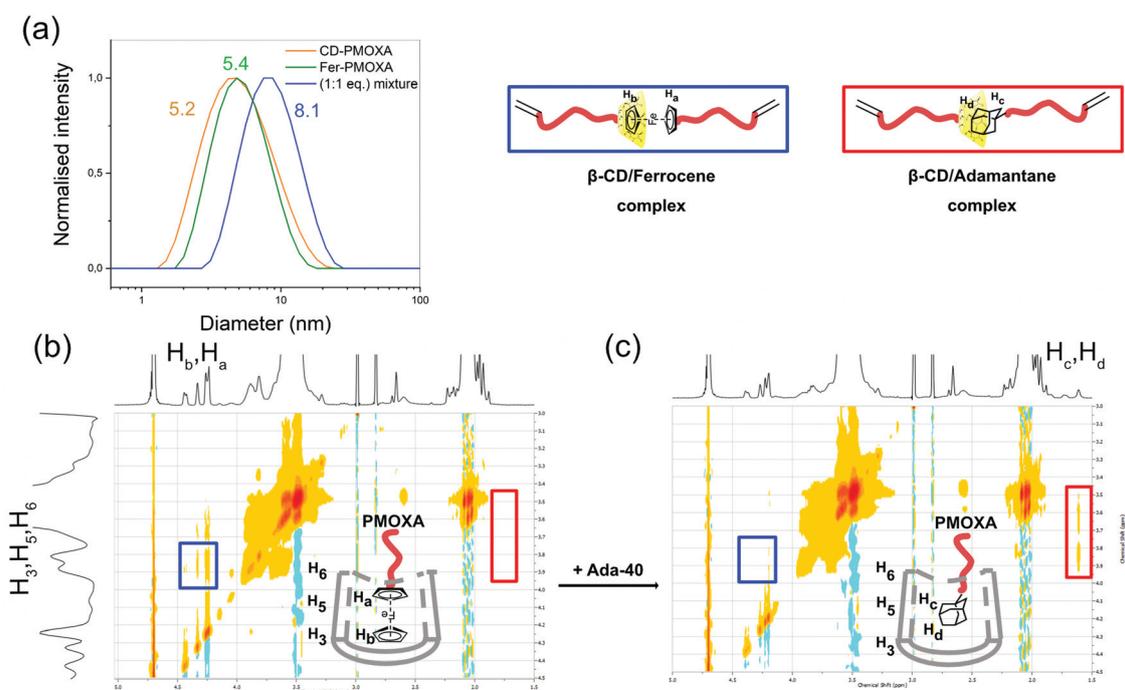
Fig. 3 (a) Size distribution of CD-PMOXA, Fer-PMOXA and their 1 : 1 molar mixture in at 25 °C ($c = 1$ g mL^{-1}). (b) 2D NOESY spectrum of 1 : 1 molar mixture of CD-PMOXA and Fer-PMOXA (5 mmol L^{-1}) in D$_2$O at 30 °C and (c) 2D NOESY spectrum after the addition of Ada-40 (Adamantane-PMOXA).

ROESY NMR were used to verify the presence of the host–guest complex (Fig. 3b and Fig. S11, S12†). A mixture of CD-PMOXA and Fer-PMOXA (1 : 1 eq.) was prepared in D_2O at 30 °C at 5 mmol L^{-1}. The ^1H NMR signals from ferrocene (H_a, H_b at $\delta = 4.17$–4.55 ppm) proved to be in resonance with the signals of the β-CD cavity protons (H_3, H_5, and H_6 at 3.55–3.80 ppm, Fig. 3b). All the respective protons associated with these signals were thus in close proximity indicating the formation of the complex and supporting the DLS data. Based on the literature, the association constant of the β-CD/adamantane complex is higher than the association constant of β-CD/ferrocene complex.[38] Therefore, the dissociation of β-CD/ferrocene complex and formation of a new host–guest complex based on the β-CD/adamantane supramolecular interaction were analysed. The previously mentioned Ada-40 from our earlier study[32] was added to the mixture of CD-PMOXA and Fer-PMOXA (1 : 1 eq.) and the NOESY 2D NMR experiments were repeated. Now the protons of adamantane (H_c, H_d at $\delta = 1.51$ ppm) were in resonance with the β-CD cavity protons (H_3, H_5, and H_6 at 3.80–3.55 ppm, red square in Fig. 3c)[32] and the previous resonance to the ferrocene protons disappeared (blue square in Fig. 3b and c). This change in protons within the β-CD cavity proved the formation of the new adamantane complex and the disappearance of the resonance signals associated with the ferrocene complex proved that it must have existed beforehand. This re-formation of the host–guest complex was used as the demonstration of the successful formation of the β-CD/ferrocene complex.

Hydrogel synthesis and characterisation

After the formation of the host–guest complex and hence the formation of the bismacromonomers as reversible cross-linkers was proved, the double cross-linked supramolecular hydrogels were prepared (Fig. 4). The hydrogels were synthesised *via* free radical polymerisation in methanol using NiPAAm (16 wt%) as the monomer, BIS (0.5 mol% or 1 mol%) as the covalent cross-linker, the host and guest bismacromonomers (0.5 mol% or 1 mol%) as the reversible redox-sensitive non-covalent cross-linker and AIBN (1 mol%) as the initiator. Prior to the hydrogel formation, the ferrocene and β-CD macromonomers were dissolved in methanol, heated at 40 °C and

stirred for 24 h for complete complex formation (Fig. S11 and S12†). Four types of double cross-linked hydrogels with different amounts of non-covalent cross-linking points (0.5 mol% or 1 mol%) and with different PMOXA chain lengths (DP 30 or 37) were prepared (Table 2). The number of supramolecular cross-linking points in the network as well as the chain length of PMOXA macromonomers allow obtaining the hydrogels with tailor-made mechanical and redox properties. After 3 days of washing with deionised water, the homogeneous and yellow ferrocene-containing hydrogels and colourless control hydrogels were obtained. All the hydrogels will be named reflecting whether they contain grafted (*G*) PMOXA chains and the DP of PMOXA chains (30 or 37) after oxidation. To determine the influence of all parameters, GH-37 with 0.5 mol% of each cross-linker was defined as the basic hydrogel (GH-37a) and the conditions were altered from there. One gel contained more permanent cross-linking units (1 mol%, GH-37b), one had more responsive cross-linking points (1 mol%, GH-37c) and the last one had shorter PMOXA chains (GH-30a). Two control hydrogels were synthesised and named accordingly as GH-35Me (with Me-35 as grafted side chains) and H-PNiPAAm (no grafted side chains). It should be noted that the chain length of PMOXA bismacromonomers as the dynamic and non-covalent cross-linker (Table 2) incorporated in the polymer network was double the original size due to the formation of the host–guest complex. The bismacromonomers hence had DP ≈74 (CD-37 and Fer-37) and DP ≈60 (CD-30 and Fer-30).

Table 2 Composition of synthesised hydrogels

Hydrogel	Type of macromonomer for host–guest complex		Permanent cross-linker BIS mol%	Host–guest cross-linker mol%
	Host	Guest		
H-PNiPAAm	—	—	0.5	—
GH-35Me	Me-35		0.5	1.0
GH-37a	CD-37	Fer-37	0.5	0.5
GH-37b	CD-37	Fer-37	1.0	0.5
GH-37c	CD-37	Fer-37	0.5	1.0
GH-30a	CD-30	Fer-30	0.5	0.5
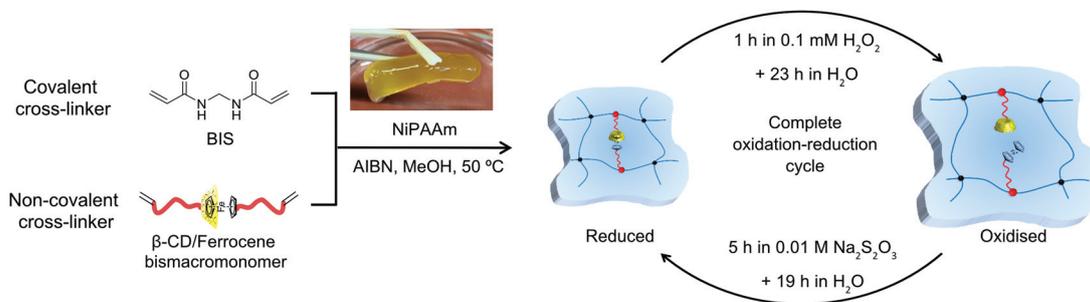
Fig. 4 Chemical structure and synthesis steps of supramolecular redox responsive ferrocene-β-CD hydrogels, including the optimised procedure to achieve fully oxidised and fully reduced hydrogels.

To study all parameters of hydrogels under suitable conditions, the oxidation and reduction process had to be optimised (Fig. 4). Treating the hydrogel with 0.25 M hydrogen peroxide (H_2O_2) did break the host–guest complex and hence reduced the degree of cross-linking of the gel which was now a grafted hydrogel cross-linked by BIS only. However, the hydrogel disintegrated over time due to side reactions induced by H_2O_2. Reducing the concentration to 0.1 mM H_2O_2 still induced the intended swelling but did not compromise the integrity of the gel. Oxidation was achieved by placing the gels for 1 h in 0.1 mM H_2O_2 and allowing them to swell for an additional 23 h in water. Choosing the correct reducing agent proved to be a challenging issue. Initial experiments with glutathione did not lead to the intended deswelling of the gel, but 0.1 M ascorbic acid did reduce the ferrocene and led to the intended deswelling of the gel. However, the deswelling was followed by strong unexpected swelling of the gel to more than 200% of the original weight. While this behavior could not be explained rationally, treating native GH-37a with 0.1 M ascorbic acid had a similar effect. Since ascorbic acid had this negative effect on the hydrogel, the conditions were changed to 10 mM sodium thiosulfate, which has been already used in the literature.[39] The following conditions proved to yield reproducible results: oxidation in 0.1 mM hydrogen peroxide for 1 h followed by an equilibration over 23 h in water to achieve full swelling. Reduction was conducted in 10 mM sodium thiosulfate and had to be carried out for at least 5 h, as kinetic measurements on GH-37c showed a complete deswelling only after a minimum of 5 h (Fig. S14†). Despite this complete macroscopic deswelling, a limited number of host–guest complexes might not have been re-formed, but had no effect on the macroscopic properties of the bulk material. In order to keep a reasonable working pattern, the whole deswelling step was elongated by placing the hydrogel in water for 19 h to a 24 h for the complete reduction step. The complete oxidation–reduction cycle was thus spread out over 48 h (Fig. 4 and Fig. S13† for a non-optimised 24 h cycle).

The difference in morphology of the supramolecular hydrogels in their optimised reduced and oxidised forms was also investigated by SEM (Fig. 5a and b). The average pore size of GH-37c increased (from 19 μm to 37 μm) when the oxidation of ferrocene in the hydrogel was carried out. This was easily reasoned that by oxidation the dissociation of host–guest complex took place and led to the swelling of hydrogel, resulting in the increase in pore size.

The optimised cycle conditions were then used to monitor the swelling degree (Q) over the reduction and oxidation cycle (Fig. 6a). Q was defined as the mass increase in % compared to the original value. Following the assumption that hydrogels consist mainly of water, the change in mass directly translated into a change in volume. On a molecular level, the distances between the permanent cross-linkers hence also increased by this percentage. The following characterisation took the values of at least 3 days washed and stored hydrogels in water after synthesis as references. All the graphs were normalised to the first swollen state (O1) as a starting point to emphasise the
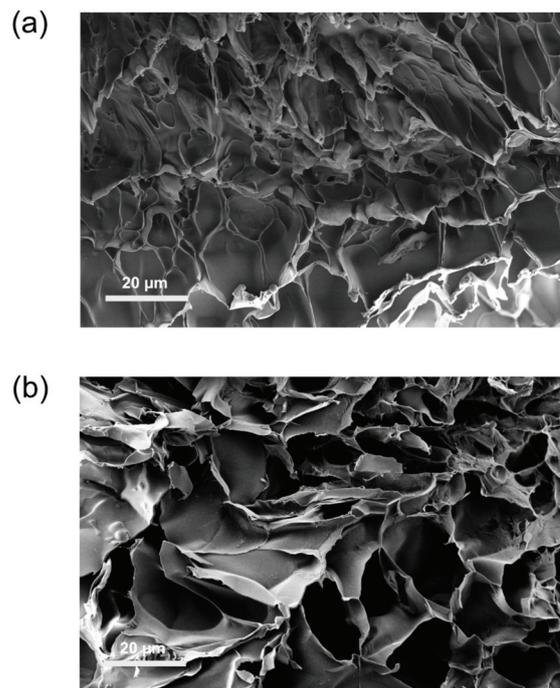
Fig. 5 (a) SEM image of GH-37c in sodium thiosulfate (reduced, scale bar 20 μm), (b) SEM image of GH-37c in hydrogen peroxide (oxidised, scale bar 20 μm).

relative differences between the gels. While GH-37a showed Q_{ox} of 8 (O1 in Fig. 6a), GH-37b showed no swelling (data not shown). The larger amount of the permanent cross-linker in GH-37b (Table 2) reduced the mesh size of the PNiPAAm network, so that the broken host–guest interactions had no macroscopic effect on the polymer upon oxidation; also no swelling in 0.1 mM H_2O_2 over 3 days was observed. For GH-37a, the hydrogel was reproducibly swelled and deswelled over 5 cycles. In comparison with GH-30a, it is apparent that the longer PMOXA chains lead to a decrease in Q of the supramolecular grafted hydrogels (GH-30a: $Q_{av.~ox.}$ = 15; GH-37a: $Q_{av.~ox.}$ = 8). This tendency could be explained as due to the longer bismacromonomer cross-linkers interconnecting the underlying PNiPAAm network more loosely than the shorter PMOXA chains. Reducing the length of the bismacromonomer complexes allowed the incorporation of cross-linking points to the network with the size similar to or less than the PNiPAAm sub-chain. This leads to the higher Q of hydrogels similar to previously reported gels using the β-CD/adamantane system.[32] With 0.5 mol% BIS in GH-37a and GH-30a, the average chain length of the PNiPAAm network in both hydrogels was expected to be about 100 units (200 C–C bonds). For GH-30a, bismacromonomers had about 180 + host–guest C–C bonds (3 bonds per repeating unit) while GH-37a had about 225 + host–guest C–C bonds for their bismacromonomers. However, the swelling and deswelling increased considerably from the third cycle for GH-30a. This hinted to a possible decomposition of the hydrogel, which could not be proved at this stage. The influence of different amounts of supramolecular cross-

(a)

(b)
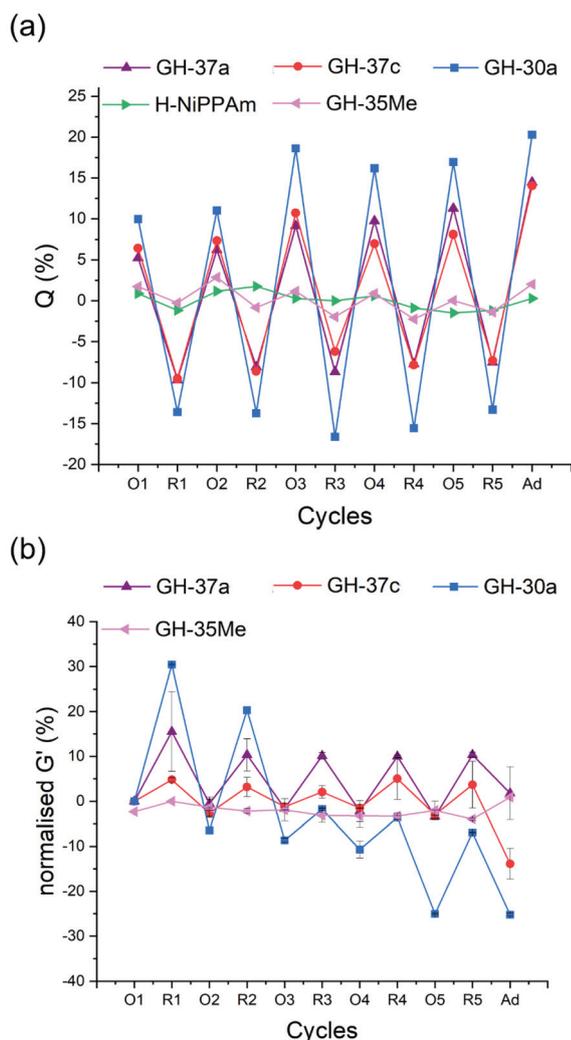
Fig. 6 (a) Swelling degree and (b) normalised storage modulus of supramolecular hydrogels GH-37a, GH-37c, GH-30a and control hydrogels H-PNiPAAm and GH-35Me. R1–R5 and O1–O5 correspond to the cycle number of reduction and oxidation, respectively.

linking points on the hydrogel properties was investigated by measuring GH-37c with 1 mol% of bismacromonomers. GH-37a and GH-37c show a constantly complete reversibility of swelling/deswelling after five redox cycles. Both hydrogels exhibited the same maximum and minimum of swelling degree in the optimised 48 h-cycle. The relative degree of swelling in the oxidised and reduced stages remain almost on the same level on each cycle for GH-37a and GH-37c (Fig. 6a).

It meant that the host–guest complexes were fully recovered after several redox cycles. It also indicated that the larger amount of responsive units did not lead to a larger response of the hydrogel (Fig. 6a), which was explained by the restrictions of the underlying PNiPAAm network as discussed for the comparison with GH-30a. To verify that specifically the supramolecular cross-linking points influenced the swelling degree of the hydrogels, the same swelling measurements of two control hydrogels (GH-35Me, H-PNiPAAm) were conducted. No differ-

ences in Q for the control hydrogels were observed upon redox cycles which confirmed the assumptions above.

At the last stage of redox cycles, the re-formation of the β-CD/ferrocene host–guest complex to β-CD/adamantane host–guest complex was used as the reference experiment to compare the number of broken cross-linking points under the influence of different stimuli (oxidation or re-forming of host–guest complex). After the last reduction process (R5 in Fig. 6a), hydrogels were placed in an aqueous solution of 2-aminoadamantane hydrochloride to form the β-CD/adamantane host–guest complex (shown in Fig. 3c through the addition of Ada-40). Forming the new complex permanently transferred the responsive double cross-linked hydrogel to a grafted hydrogel without any dynamic cross-linking points (Fig. 6a, "Ad" entry). Both the supposedly intact hydrogels GH-37a and GH-37c showed a defined increase in swelling once adamantane completely replaced the ferrocene in the complex (Q of 14 instead of 8 for both GH-37a and GH-37c). Despite the different amounts of host–guest complexes, both gels showed the same increase in Q (about 15) when treated with adamantane. This was in line with the restrictions imposed by the base PNiPAAm network already discussed. GH-30a, however, showed a similar swelling when treated with adamantane as in the oxidation–reduction cycles 3–5 of GH-30a when the suggested decomposition started.

In addition to the swelling degree measurements, the rheology of the synthesised hydrogels was investigated. Elastic deformation of the hydrogels was investigated by the storage modulus G' following a frequency sweep (see section 7 including Fig. S15 of the ESI† for details). Fig. 6b shows the normalised values of storage modulus after several reduction and oxidation cycles for GH-37a, GH-37c, and GH-30a and the GH-35Me as the control hydrogel. In order to compare all gels, the values were normalised on the first swelling cycle (no host–guest interactions) as the base value. The reduction of supramolecular hydrogels led to an increase of the storage modulus while the oxidation led to a decrease of the storage modulus. The rheological data were very much consistent with the observed trends in the swelling degree measurements. As expected, the control gel GH-35Me showed no increase or decrease in the oxidation–reduction cycles. GH-37a and GH-37c showed a reproducible decrease and increase in stiffening over all oxidation–reduction cycles. Very much unexpected, GH-37a showed the larger amplitude (10–15%) than GH-37c (about 5%).In contrast, GH-37a was weakened to a similar value of the first swelling after adamantane was added, but GH-37c was weakened to −15% of the first swelling cycle. This indicated that the larger amount of ferrocene in GH-37c led to more structural defects in the hydrogel. Breaking all host–guest interactions with the addition of adamantane then exposed these structural defects. Due to the shorter length of PMOXA, GH-30a showed a large increase in amplitude up to 30% of the reference value for GH-35Me. At the same time, the large difference in swelling and deswelling for GH-30a was constant (Fig. 6a), the G' began to decline rapidly over the following cycles (Fig. 6b), going down to −25% of the reference

value. This decline underlined the assumption of a decomposition of the hydrogel during the repeated redox cycles which was already hinted in the swelling data discussed earlier. Since this decomposition only occurred with the shortest PMOXA chain, it hinted that the valence electrons of ferrocene can interfere with the radical polymerisation leading to a less stable hydrogel with more structural defects. When the PMOXA was long enough to wrap ferrocene, this interference was suppressed in GH-37a but surfaced again in GH-37c when more ferrocene was present in the system. Summarising the results from swelling measurement, rheology and SEM, it is arguable that the presence of supramolecular cross-linking points based on the β-CD/ferrocene complex in the hydrogel structure leads to a significant, reproducible and reversible redox sensitivity.

Conclusions

In this study, novel redox-sensitive double cross-linked supramolecular hydrogels based on the host–guest interaction between β-cyclodextrin and ferrocene in a polymer chain network were synthesised. These hydrogels benefit from a combination of covalent and redox responsive non-covalent network joints (*i.e.* cross-linking points), which allowed combining of the properties of physical and chemical cross-linking points. β-CD or ferrocene units were introduced using modified PMOXA macromonomers. After the formation of the complex, the PMOXA chains had polymerisable units on both ends, effectively forming responsive bismacromonomers for a copolymerisation with NiPAAm. A shorter version (DP = 30) and a longer version (DP = 37) of clearly defined PMOXA macromonomers (CD-PMOXA and Fer-PMOXA) have been synthesised and thoroughly characterised by ^{1}H NMR, GPC, FTIR and Raman spectroscopy. The complexation study provided by DLS and 2D NOESY and ROESY NMR confirmed the formation of a bismacromonomer composed of a 1:1 host–guest complex. The resulting supramolecular hydrogel then contained the PMOXA chains with the β-CD/ferrocene complex as a reversible bismacromonomer cross-linker and BIS as a permanent cross-linker, which resulted in the intended double cross-linked hydrogels. These hydrogels show significant redox-sensitive properties compared to hydrogels without host–guest interactions. Both their weight and their elastic modulus responded reproducibly over various cycles to change from an oxidising to a reducing environment and *vice versa*. Increasing the amount of supramolecular cross-linking points in the hydrogel as well as decreasing the chain length of bismacromonomers demonstrated how the influence of the host–guest complex can be fine-tuned. While increasing the amount of the β-CD/ferrocene complex did increase the magnitude in response to the swelling, the rheological response revealed the existence of structural defects. Decreasing the molar mass of the bismacromonomers led to an increase in swelling degree and changes in elastic moduli of the supramolecular grafted hydrogels (GH-30a and GH-37a). However, since the ferrocene did interfere with the radical polymerisation, hydrogels with shorter bismacromonomers or an increased content of the bismacromonomer increased the amount of structural defects of the network. The possibility to control the properties of hydrogels with the β-CD/ferrocene complex as reversible cross-linking points makes this system a promising one for various applications in microfluidics, for example, as a chemical actuator or sensor, in diagnostics, and for capturing or releasing specific molecules upon redox changes in the environment.

Author contributions

Nikolai Liubimtsev: methodology, investigation, data curation, formal analysis, writing – original draft, visualisation. Tom Kösterke: methodology, investigation, data curation, validation, formal analysis, writing – review and editing, visualisation. Yunjiao Che: conceptualisation, methodology, investigation. Dietmar Appelhans: conceptualisation, resources, writing – review and editing, supervision, funding acquisition. Jens Gaitzsch: conceptualisation, methodology, formal analysis, writing – review and editing, visualisation, supervision, project administration. Brigitte Voit: conceptualisation, resources, writing – review and editing, supervision, project administration, funding acquisition.

Conflicts of interest

There are no conflicts to declare.

Acknowledgements

References

1 A. Döring, W. Birnbaum and D. Kuckling, *Chem. Soc. Rev.*, 2013, **42**, 7391–7420.
2 M. Mahinroosta, Z. Jomeh Farsangi, A. Allahverdi and Z. Shakoori, *Mater. Today Chem.*, 2018, **8**, 42–55.
3 H. S. Choi and N. Yui, *Prog. Polym. Sci.*, 2006, **31**, 121–144.
4 Y. L. Zhao and J. Fraser Stoddart, *Langmuir*, 2009, **25**, 8442–8446.
5 T. Miyata, N. Asami and T. Uragani, *Nature*, 1999, **399**, 766–768.
6 A. B. W. Brochu, S. L. Craig and W. M. Reichert, *J. Biomed. Mater. Res., Part A*, 2011, **96**, 492–506.
7 D. Melekaslan, F. Kasapoglu, K. Ito, Y. Yagci and O. Okay, *Polym. Int.*, 2004, **53**, 237–242.

8 M. I. Bhatti and A. Mohyuddin, *Annu. Rev. Biomed. Eng.*, 2014, **2**, 3–4.

9 J. M. Zayed, N. Nouvel, U. Rauwald and O. A. Scherman, *Chem. Soc. Rev.*, 2010, **39**, 2806–2816.

10 T. Xiao, L. Xu, L. Zhou, X. Q. Sun, C. Lin and L. Wang, *J. Mater. Chem. B*, 2019, **7**, 1526–1540.

11 B. W. Liu, H. Zhou, S. T. Zhou and J. Y. Yuan, *Eur. Polym. J.*, 2015, **65**, 63–81.

12 T. Kakuta, Y. Takashima and A. Harada, *Macromolecules*, 2013, **46**, 4575–4579.

13 Y. Takashima, S. Hatanaka, M. Otsubo, M. Nakahata, T. Kakuta, A. Hashidzume, H. Yamaguchi and A. Harada, *Nat. Commun.*, 2012, **3**, 1270.

14 M. Nakahata, Y. Takashima, A. Hashidzume and A. Harada, *Angew. Chem., Int. Ed.*, 2013, **52**, 5731–5735.

15 T. F. A. De Greef, M. M. J. Smulders, M. Wolffs, A. P. H. J. Schenning, R. P. Sijbesma and E. W. Meijer, *Chem. Rev.*, 2009, **109**, 5687–5754.

16 R. Tong, L. Wang, H. Yu, Zain-ul-Abdin, H. Khalid, M. Akram and Y. Chen, *J. Inorg. Organomet. Polym. Mater.*, 2015, **25**, 1053–1059.

17 D. Schmitz and A. Pich, *Polym. Chem.*, 2016, **7**, 5687–5697.

18 M. Arslan, M. A. Tasdelen, T. Uyar and Y. Yagci, *Eur. Polym. J.*, 2015, **71**, 259–267.

19 M. Nakahata, Y. Takashima, H. Yamaguchi and A. Harada, *Nat. Commun.*, 2011, **2**, 511–516.

20 Y. Suzaki, T. Taira and K. Osakada, *J. Mater. Chem.*, 2011, **21**, 930–938.

21 Y. H. Ko, I. Hwang, D. W. Lee and O. Kim, *Isr. J. Chem.*, 2011, **51**, 506–514.

22 J. M. Sturtevant, *Proc. Natl. Acad. Sci. U. S. A.*, 1977, **74**, 2236–2240.

23 W. S. Jeon, K. Moon, S. H. Park, H. Chun, Y. H. Ko, J. Y. Lee, E. S. Lee, S. Samal, N. Selvapalam, M. V. Rekharsky, V. Sindelar, D. Sobransingh, Y. Inoue, A. E. Kaifer and K. Kim, *J. Am. Chem. Soc.*, 2005, **127**, 12984–12989.

24 S. Moghaddam, C. Yang, M. Rekharsky, Y. H. Ko, K. Kim, Y. Inoue and M. K. Gilson, *J. Am. Chem. Soc.*, 2011, **133**, 3570–3581.

25 J. Wu, L. Wang, H. Yu, Zain-ul-Abdin, R. U. Khan and M. Haroon, *J. Organomet. Chem.*, 2017, **828**, 38–51.

26 M. Nakahata, Y. Takashima and A. Harada, *Angew. Chem., Int. Ed.*, 2014, **53**, 3617–3621.

27 A. Harada and S. Takahashi, *J. Inclusion Phenom.*, 1984, **2**, 791–798.

28 A. Harada and S. Takahashi, *J. Chem. Soc., Chem. Commun.*, 1984, 645–646.

29 D. Osella, A. Carretta, C. Nervi, M. Ravera and R. Gobetto, *Organometallics*, 2000, **19**, 2791–2797.

30 L. Peng, H. Zhang, A. Feng, M. Huo, Z. Wang, J. Hu, W. Gao and J. Yuan, *Polym. Chem.*, 2015, **6**, 3652–3659.

31 Y. F. Wang, D. L. Zhang, T. Zhou, H. S. Zhang, W. Z. Zhang, L. Luo, A. M. Zhang, B. J. Li and S. Zhang, *Polym. Chem.*, 2014, **5**, 2922–2927.

32 Y. Che, J. Gaitzsch, N. Liubimtsev, S. Zschoche, T. Bauer, D. Appelhans and B. Voit, *Soft Matter*, 2020, **16**, 6733–6742.

33 Y. Che, S. Zschoche, F. Obst, D. Appelhans and B. Voit, *J. Polym. Sci., Part A: Polym. Chem.*, 2019, **57**, 2590–2601.

34 N. Adams and U. S. Schubert, *Adv. Drug Delivery Rev.*, 2007, **59**, 1504–1520.

35 F. C. Gaertner, R. Luxenhofer, B. Blechert, R. Jordan and M. Essler, *J. Controlled Release*, 2007, **119**, 291–300.

36 A. Groß, G. Maier and O. Nuyken, *Macromol. Chem. Phys.*, 1996, **197**, 2811–2826.

37 J. M. Casas-Solvas, A. Vargas-Berenguel, L. F. Capitán-Vallvey and F. Santoyo-González, *Org. Lett.*, 2004, **6**, 3687–3690.

38 A. Harada, Y. Takashima and M. Nakahata, *Acc. Chem. Res.*, 2014, **47**, 2128–2140.

39 Z. Wang, H. Mohwald and C. Gao, *Langmuir*, 2011, **27**, 1286–1291.